Lyapunov Redesign for Interleaved Boost Converter in PV-Based DC Microgrids

Aqeel Ur Rahman*, Filippo Pellitteri†, Georgios Tzounas*
*School of Electrical and Electronic Engineering, University College Dublin, Dublin, Ireland
†Dept. of Engineering, University of Palermo, Palermo, Italy
aqeel.urrahman@ucd.ie, filippo.pellitteri@unipa.it, georgios.tzounas@ucd.ie

***Abstract*—This paper presents a Lyapunov-redesign-based control for a three-phase interleaved boost converter (IBC) interfacing photovoltaic (PV) systems with a dc microgrid. IBCs are attractive due to their low current ripple and high power density, although their multiphase structure also introduces the need for a means of balancing current sharing among the converter phases. The proposed control law, which generates independent per phase switching signals, achieves effective current sharing while ensuring large-signal stability of the closed-loop system. Comparative analysis with a conventional boost converter (CBC) confirms lower current and voltage ripple. The performance of the proposed control is validated through MATLAB/Simulink simulations and controller-hardware-in-the-loop (C-HIL) real-time tests using a Typhoon HIL 404 platform and a TI C2000 microcontroller.**

***Index Terms*—PV integration, Nonlinear control multiphase dc-dc converter, dc microgrids, Lyapunov redesign, large-signal stability.**

I. Introduction

A. Motivation

The growing deployment of renewable energy sources has increased the adoption of dc microgrids, where dc-dc converters serve as the primary interface for power conversion and voltage regulation. Effective control design is essential to fully exploit the advantages of modern converters, such as interleaved structures, and ensure reliable power conversion. Linear controllers are typically designed around a predefined operating point and may therefore exhibit poor dynamic performance when operating conditions vary, as is common in dc microgrids. Nonlinear controllers offer greater flexibility, but usually present higher design complexity. This paper aims to address this trade-off by proposing a Lyapunov-redesign-based controller for a three-phase interleaved boost converter that maintains low complexity while ensuring large-signal stability.

B. Literature Review

Photovoltaic (PV) systems are the most widely used renewable energy sources, particularly in dc microgrids, which provide reduced transmission losses and the ability to handle multivoltage-level system architectures [1]–[4]. Integration between PV systems and the microgrid involves the use of dc–dc boost converters that increase the low output voltage produced by PV modules to the bus voltage required by the load [5]. However, when the voltage-gain demand is high, a conventional boost converter (CBC) must operate at extreme duty cycles, which subjects the switching device to excessive voltage stress, increases diode reverse-recovery losses, and ultimately degrades conversion efficiency [6].

To overcome these issues, interleaved boost converters (IBCs) have been introduced, where multiple converter phases run in parallel with phase-shifted switching signals [7]. This topology naturally decreases input current ripple, reduces electromagnetic interference, and increases both efficiency and power density over a single-stage converter [8]. However, this configuration introduces complexities such as current balancing and control synchronization.

The nonlinear behavior of the system further complicates control design, rendering traditional linear controllers such as proportional-integral (PI) regulators less effective [9]. Consequently, several nonlinear and intelligent control techniques have been proposed to improve dynamic performance, particularly under load transients and irradiance variations [10]–[14]. For instance, sliding-mode control [15] provides robustness to parameter variations but also introduces chattering, while a switched controller [16] can improve transient performance but lacks large-signal stability guarantees. Machine-learning-based strategies, such as fuzzy [17] neural network-based model predictive control and deep reinforcement learning [18], have also been explored; however, they depend on extensive offline training, and their computational burden limits real-time applicability. Despite these efforts, a low-complexity nonlinear control approach that preserves system dynamics while ensuring current balancing in multiphase interleaved converters has not been adequately addressed.

C. Contribution

The contributions of this paper are as follows:

1) A Lyapunov-redesign-based cascaded controller is proposed for a three-phase IBC for maximum power point tracking (MPPT) and current balancing, ensuring global stability of the closed-loop system under model assumptions.
2) The corresponding closed-loop system is compared with a conventional boost-converter-based system employing the same controller, demonstrating lower output ripple and reduced passive component size.

This work is supported by Research Ireland/SFI, under grant number 21/SPP/3756 through the NexSys Strategic Partnership Programme.

3) The proposed controller is validated through MATLAB/Simulink simulations and real-time controller hardware-in-loop (C-HIL) experiments using a Typhoon HIL 404 platform and a TI C2000 microcontroller.

D. Paper Organization

The remainder of this paper is organized as follows. Section II describes the state-space model used for the control design. Section III introduces the proposed nonlinear controller based on Lyapunov redesign, along with the stability analysis of the closed-loop system. Simulation and experimental results are presented and discussed in Section IV. Finally, conclusions are duly drawn in Section V.

II. Mathematical Modeling

This section presents the averaged state-space model of a three-phase IBC interfacing a PV source with a dc microgrid, which forms the basis for the control design in Section III.

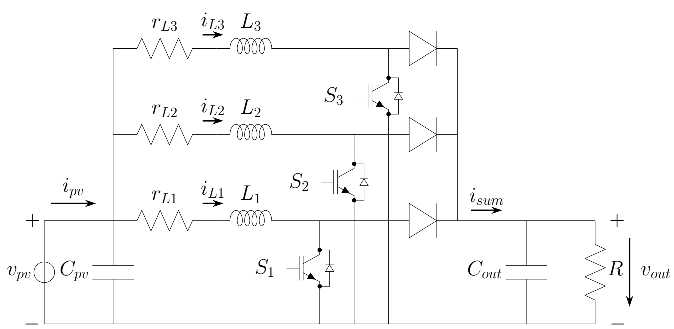

Fig. 1: Schematic diagram of a three-phase IBC.

The configuration of a three-phase IBC supplied by a PV panel is shown in Fig. 1. The system variables are defined as follows: v_{pv} is the PV terminal voltage, i_{Lj} with $j = 1, 2, 3$ is the inductor current of the j^{th} phase, and v_{out} is the output voltage. The variable i_{sum} represents the sum of all phase currents $i_{sum} = \sum_{j=1}^{3} i_{Lj}$. Under the assumption of continuous-conduction-mode operation, the switching action of each phase is represented by its average duty ratio $u_j \in [0, 1]$. to obtain a model suitable for control design. The averaged state-space equations are given by:

$$C_{pv} v'_{pv} = i_{pv} - \sum_{j=1}^{3} i_{Lj} \quad (1)$$

$$L_j i'_{Lj} = -r_{Lj}\, i_{Lj} - (1 - u_j)\, v_{out} + v_{pv}, \quad j = 1, 2, 3 \quad (2)$$

$$C_{out} v'_{out} = \sum_{j=1}^{3} (1 - u_j)\, i_{Lj} - \frac{1}{R}\, v_{out} \quad (3)$$

Here, i_{pv} is the output current of the PV panel, which depends on the terminal voltage v_{pv} through the PV I-V characteristic. In the model, i_{pv} is treated as a measured variable at each sampling instant rather than an explicit function of v_{pv}. C_{pv} is the input-side capacitance that smooths fluctuations in the PV voltage, L_j and r_{Lj} are the inductance and parasitic resistance of the j^{th} phase, C_{out} is the output capacitance, and R is the equivalent load resistance. The control inputs u_j represent the duty cycle of each phase.

The averaged state-space model above is used for control derivation, as this is the standard approach for designing nonlinear controllers. The derived control law is then verified on the switched model in simulation with a fixed time step. For simplification, a resistive load is considered, which does not capture the full dynamics of a dc microgrid. However, since the proposed controller does not depend on load dynamics, it can be extended to other case studies of dc microgrids such as constant power loads, electric vehicle integration, and different power sources. Moreover, the redesign control part also addresses only nominal part and it can be extended to handle uncertainties.

III. Lyapunov Redesign

A hierarchical two-loop control strategy is implemented for the three-phase IBC interfacing a PV source with a dc microgrid. The outer loop regulates the voltage of the PV terminal v_{pv} to ensure maximum power tracking, while the inner loop tracks the inductor current references using Lyapunov redesign. The output voltage v_{out} is indirectly regulated through the power balance between input and output. The control structure is shown in Fig. 2.

The stability analysis of both loops relies on the following standard result:

Lemma (Lyapunov Stability) [19]: Let $e = 0$ be an equilibrium point. If there exists a continuously differentiable function $V(e) > 0$ for all $e \neq 0$, with $V(0) = 0$, such that $V'(e) \leq -\alpha\, V(e)$ for some $\alpha > 0$, then the equilibrium $e = 0$ is globally exponentially stable, and $\|e(t)\| \leq \|e(0)\|\, e^{-\frac{\alpha}{2} t}$.

Outer PV Voltage Control Loop: The outer loop ensures that the PV voltage v_{pv} tracks the reference $v_{pv,ref}$, which is provided by an MPPT algorithm. Define the voltage tracking error:

$$e_v = v_{pv,ref} - v_{pv} \quad (4)$$

Differentiating (4) and substituting from (1):

$$e'_v = v'_{pv,ref} - \frac{1}{C_{pv}} \left(i_{pv} - \sum_{j=1}^{3} i_{Lj} \right) \quad (5)$$

Choose the Lyapunov candidate $V_v = \frac{1}{2} e_v^2$, whose time derivative is $V'_v = e_v\, e'_v$. To enforce $V'_v < 0$, the desired error dynamics are chosen as $e'_v = -k_v\, e_v$, where $k_v > 0$ is the outer-loop control gain. This choice yields $V'_v = -k_v\, e_v^2 < 0$, ensuring exponential convergence of the voltage tracking error.

In the proposed implementation, $v'_{pv,ref}$ is set to zero without affecting the closed-loop stability, as the feedback term $k_v\, e_v$ compensates for the resulting tracking error. In practical MPPT applications, this is further justified since $v_{pv,ref}$ is piecewise constant and $v'_{pv,ref} = 0$ between perturbation instants. Substituting (5) into $e'_v = -k_v\, e_v$ and solving for the total inductor current reference $i_{ref} = \sum_{j=1}^{3} i_{Lj}$, the following control law is obtained:

$$i_{ref} = i_{pv} - C_{pv} \left(v'_{pv,ref} + k_v\, e_v \right) \quad (6)$$

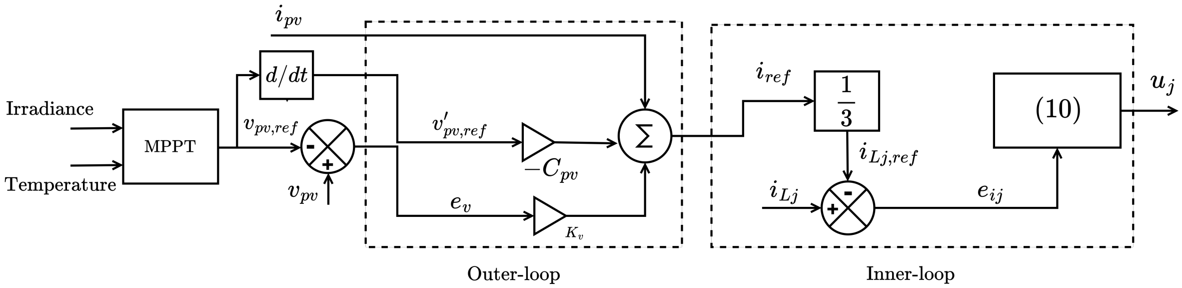

Fig. 2: Block diagram of proposed control.

This reference is equally distributed among the three phases:

$$i_{Lj,ref} = \frac{i_{ref}}{3}, \quad j = 1, 2, 3 \tag{7}$$

Inner Current Control Loop: Each inductor current i_{Lj} tracks its reference $i_{Lj,ref}$ using a Lyapunov-based controller. Define the current tracking error:

$$e_{ij} = i_{Lj,ref} - i_{Lj} \tag{8}$$

Differentiating (8) and substituting from (2):

$$e'_{ij} = i'_{Lj,ref} - \frac{1}{L_j}\left(-r_{Lj}\, i_{Lj} - (1-u_j)\, v_{out} + v_{pv}\right) \tag{9}$$

Choose the Lyapunov candidate $V_{ij} = \frac{1}{2}e_{ij}^2$, with $V'_{ij} = e_{ij}\, e'_{ij}$. To guarantee $V'_{ij} < 0$, the desired error dynamics are chosen as $e'_{ij} = -k_i\, e_{ij}$, where $k_i > 0$ is the inner-loop control gain. This yields $V'_{ij} = -k_i\, e_{ij}^2 < 0$, ensuring exponential convergence of each current tracking error. Substituting (9) into $e'_{ij} = -k_i\, e_{ij}$ and solving for u_j, the control input is derived as:

$$u_j = 1 - \frac{-r_{Lj}\, i_{Lj} + v_{pv} - L_j\left(i'_{Lj,ref} + k_i\, e_{ij}\right)}{v_{out}} \tag{10}$$

Note that (10) requires $v_{out} \neq 0$, which is satisfied under normal operating conditions since the output voltage remains strictly positive.

Stability Analysis: Under the control laws (6) and (10), the closed-loop error dynamics become:

$$e'_v = -k_v\, e_v \tag{11}$$

$$e'_{ij} = -k_i\, e_{ij} \tag{12}$$

To analyze the overall system stability, define a composite Lyapunov function:

$$V = \frac{1}{2}\, e_v^2 + \frac{1}{2}\sum_{j=1}^{3} e_{ij}^2 \tag{13}$$

Its time derivative along the closed-loop trajectories is:

$$V' = -k_v\, e_v^2 - k_i \sum_{j=1}^{3} e_{ij}^2 \leq -\gamma\, V \tag{14}$$

TABLE I: PV and IBC parameters and values.

PV Panel	
Parallel and series strings	4×4
v_{oc}	36.3 V
i_{sc}	7.8 A
Cells per module	60
v_{mp}	29 V
IBC Parameters	
Input capacitance C_{pv}	200 μF
Inductance L_j	1.8 mH
Internal resistance r_{Lj}	1 mΩ
Output capacitance C_{out}	250 μF

where $\gamma = 2\,\min(k_v,\, k_i) > 0$. By the Lemma, the origin of the composite error space $(e_v, e_{i1}, e_{i2}, e_{i3}) = \mathbf{0}$ is globally exponentially stable under model assumptions, with the convergence bound:

$$V(t) \leq V(0)\, e^{-\gamma\, t} \tag{15}$$

This guarantees that all tracking errors decay exponentially to zero, with the rate of convergence governed by γ. The gains k_v and k_i are selected through iterative tuning based on the desired error dynamics, and serve a dual role: ensuring stability and shaping the transient response. Selecting $k_i \gg k_v$ enforces a time-scale separation between the fast inner current loop and the slower outer voltage loop, which is consistent with the cascaded control architecture.

IV. Results and Discussion

The performance of the proposed Lyapunov-based nonlinear controller for the IBC is evaluated in a closed-loop configuration under time-domain simulations, using MATLAB/Simulink. The simulation parameters are given in Table I.

The simulation results are summarized in Fig. 3, which shows the system response under varying operating conditions. Fig. 3a shows the converter output power profile. Fig. 3b illustrates the MPPT tracking of the PV voltage; the black dotted line represents the time-varying reference provided by the MPPT algorithm, and the solid black line is the actual PV voltage. As shown in the figure, the PV voltage accurately tracks the reference. The zoomed-in sections illustrate the transient and steady-state responses.

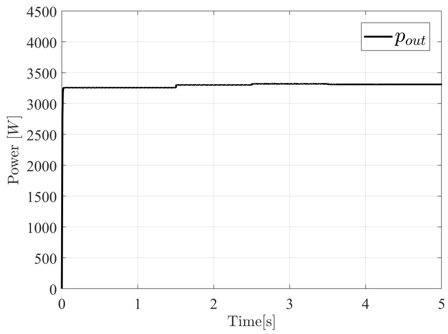

(a) Output power P_{out}

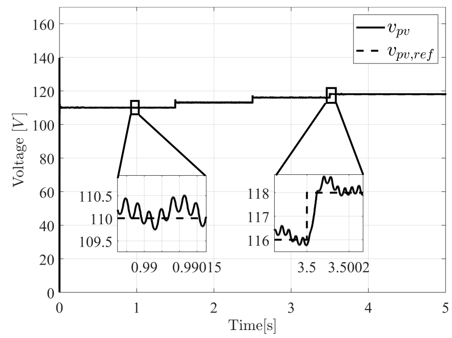

(b) MPPT tracking of v_{pv}

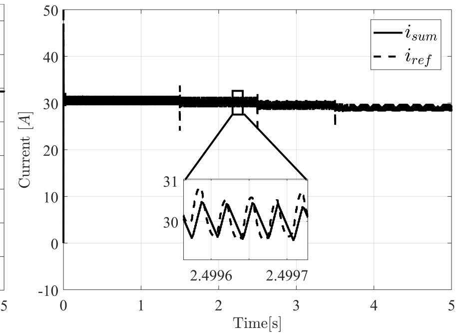

(c) Current tracking for inner-loop control

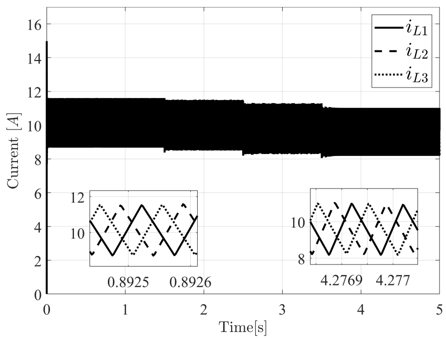

(d) Phase-shifted current in each inductor leg

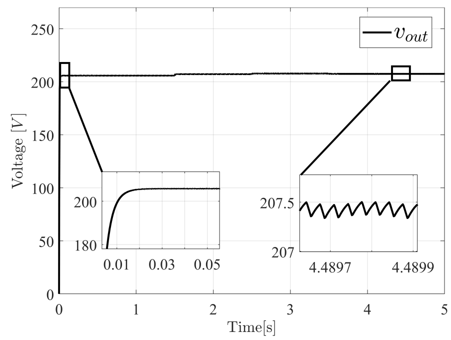

(e) Output voltage response

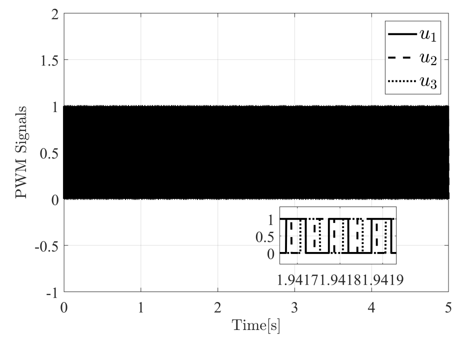

(f) Phase-shifted PWM signals

Fig. 3: Simulation results of the IBC using a cascaded nonlinear controller.

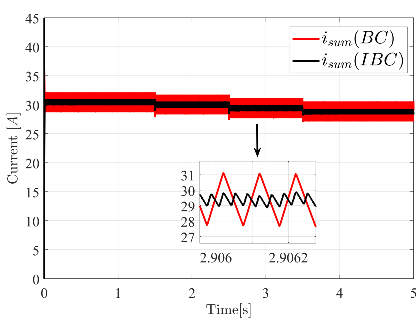

(a) Inductor current ripple comparison

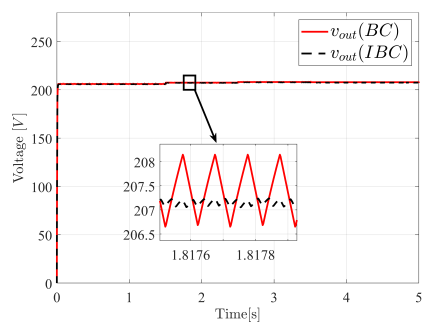

(b) Comparison of output voltage ripple

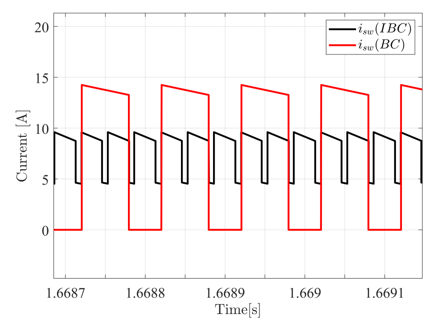

(c) Comparison of switched current

Fig. 4: Comparative analysis of the IBC and a CBC.

The inner-loop controller is responsible for accurate current tracking. The proposed controller tracks the optimal current trajectory, as shown in Fig. 3c.

Fig. 3d shows the current through each inductor, distinguished by three different line styles for clarity. Under different time-varying reference conditions, the waveforms of the individual currents are phase-shifted in a balanced manner despite parameter variations across the phases. The results confirm the effectiveness of the proposed controller in terms of current balancing.

Fig. 3e and Fig. 3f present the output voltage response and the applied PWM signals. The zoomed-in sections of the voltage graph show the transient response and the transition between different output voltage phases. Similarly, the zoomed-in section of the PWM signals shows the phase-

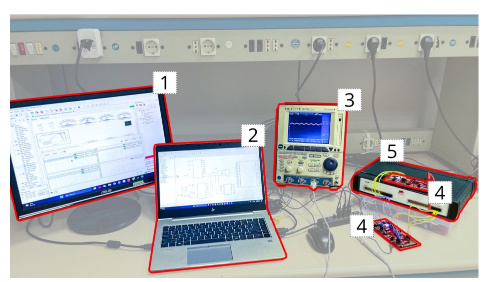

Fig. 5: C-HIL experimental test bench.

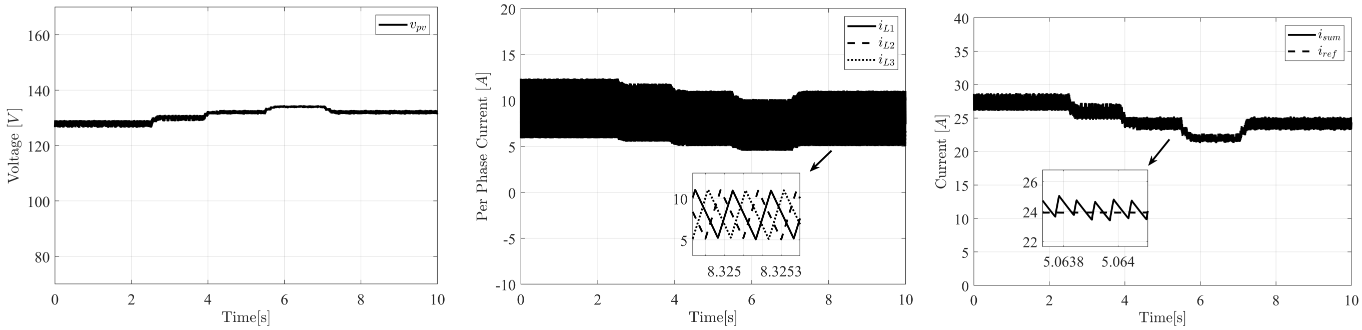

(a) PV voltage response under C-HIL test (b) Per-phase current response under C-HIL test (c) Tracking of total current under C-HIL test

Fig. 6: C-HIL test results for the IBC.

shifted PWM signals applied to the IBC through switches S_1, S_2, and S_3. The gain values of the proposed controller are tuned through iterative simulation and are set to $k_v = 2$ and $k_i = 5000$.

A. Comparative Analysis

The IBC topology is compared with a CBC in terms of inductor current ripple, output voltage ripple, and switching current. Fig. 4 presents the overall comparative analysis. It is evident from Fig. 4a that the IBC exhibits a lower ripple percentage than the CBC.

The output voltage response also favors the IBC; with proper control, it exhibits a lower voltage ripple. The comparative graph of output voltage (Fig. 4b) shows that the IBC has a lower voltage ripple than a CBC for the same output capacitance, indicating that the output capacitor size can be reduced. The switching current i_{sw} is measured immediately after the switch. A comparison of the switching current for both topologies is presented in Fig. 4c.

B. C-HIL Experimental Test

The proposed control scheme is further validated using a C-HIL test bench for real-time verification. The power stage, including the PV panel and the three-phase IBC, is emulated on the Typhoon HIL 404 real-time emulator, while the nonlinear control algorithm is deployed on a TI C2000 LAUNCHXL-F28379D microcontroller. The microcontroller receives the measured state variables (v_{pv}, i_{Lj}, v_{out}) from the Typhoon emulator via analog-to-digital converter channels and sends the computed PWM switching signals (S_1, S_2, S_3) back to the emulator. This configuration forms a closed-loop real-time test environment. Fig. 5 shows the complete C-HIL setup. A second LAUNCHXL-F28379D board is used for auxiliary signal acquisition. The supervisory control and data acquisition (SCADA) panel provides real-time monitoring and allows the operator to vary the operating conditions during the test. The host PC is used to design the power stage schematic in the Typhoon schematic editor and to program the control code on the microcontroller.

For the C-HIL test, it is assumed that the MPPT reference voltage $v_{pv,ref}$ is pre-computed for known temperature and irradiance profiles and provided directly to the outer voltage loop. The converter and control parameters are the same as those used in the simulation (Table I). Fig. 6 summarizes the C-HIL results, organized into three subfigures that illustrate the performance of the proposed control algorithm in real time. The response of the PV voltage is shown in Fig. 6a; the step changes in the reference value correspond to variations in weather conditions, and the controller successfully tracks each transition. Figs. 6b and 6c show the current balance per phase and the output current tracking, respectively. The zoomed-in sections of the figures provide a detailed view of both the balanced phase currents and the reference tracking behavior. The accurate current tracking confirms the effectiveness of the Lyapunov-based inner-loop control algorithm under real-time operating conditions. The C-HIL results are in close agreement with the simulation results presented in Section IV, which confirms the practical applicability of the proposed controller.

V. Conclusion

This paper presented a Lyapunov-based nonlinear control strategy for a three-phase interleaved boost converter in PV-based dc microgrids. The interleaved converter topology offers advantages such as reduced current ripple, wide operating range, and high power-transfer capability; however, these advantages are contingent on proper control design. A cascaded two-loop control law was derived using Lyapunov redesign method, where the outer loop ensures MPPT voltage tracking and the inner loop guarantees current tracking and balanced phase-current distribution. Global exponential stability of the closed-loop system was formally established through a composite Lyapunov function.

Simulation results demonstrated the effectiveness of the proposed method under time-varying weather conditions. Furthermore, the comparative analysis between the proposed system (IBC with nonlinear control) and a conventional boost converter confirmed lower current and voltage ripple. Finally, C-HIL experimental results using a Typhoon HIL 404 platform and a TI C2000 microcontroller validated the real-time applicability of the proposed controller and showed close agreement with the simulation results.

Future work includes extending the proposed control framework to address phase-failure conditions and determining optimal phase shifts under more realistic dc microgrid case studies.

REFERENCES

[1] T. Thomas, M. K. Mishra, C. Kumar, and M. Liserre, "Control of a PV-Wind Based DC Microgrid With Hybrid Energy Storage System Using Lyapunov Approach and Sliding Mode Control," *IEEE Transactions on Industry Applications*, vol. 60, no. 2, pp. 3746–3758, 2024.

[2] P. Roy, J. He, T. Zhao, and Y. V. Singh, "Recent Advances of Wind-Solar Hybrid Renewable Energy Systems for Power Generation: A Review," *IEEE Open Journal of the Industrial Electronics Society*, vol. 3, pp. 81–104, 2022.

[3] J. Hu, Y. Shan, K. W. Cheng, and S. Islam, "Overview of Power Converter Control in Microgrids—Challenges, Advances, and Future Trends," *IEEE Transactions on Power Electronics*, vol. 37, no. 8, pp. 9907–9922, 2022.

[4] A. Ur Rahman, N. Campagna, F. Pellitteri, A. Oscar Di Tommaso, and R. Miceli, "Stability-Centric Design of a Droop-Mounted Adaptive Nonlinear Control for EV Charging in DC Microgrid," *IEEE Access*, vol. 12, pp. 123 362–123 375, 2024.

[5] S. A. Q. Mohammed and J.-W. Jung, "A State-of-the-Art Review on Soft-Switching Techniques for DC–DC, DC–AC, AC–DC, and AC–AC Power Converters," *IEEE Transactions on Industrial Informatics*, vol. 17, no. 10, pp. 6569–6582, 2021.

[6] B. S. Revathi and M. Prabhakar, "Solar PV Fed DC Microgrid: Applications, Converter Selection, Design and Testing," *IEEE Access*, vol. 10, pp. 87 227–87 240, 2022.

[7] L. G. Fernandes, J. W. M. Soares, D. F. Cortez, and A. A. Badin, "Multiphase Interleaved Boost Converter With Frequency Modulation for Sensorless Current Sharing," *IEEE Transactions on Industrial Electronics*, vol. 72, no. 6, pp. 5846–5856, 2025.

[8] P. Arvind, G. H. Raghav, and M. Prabhakar, "Design and Development of a Versatile Interleaved Boost Converter for PV Applications," in *2025 16th Power Electronics, Drive Systems, and Technologies Conference (PEDSTC)*. IEEE, 2025, pp. 1–5.

[9] F. Pellitteri, N. Campagna, R. Inguanta, and R. Miceli, "Application of a Multiphase Interleaved DC-DC Converter for Power-to-Hydrogen Systems," in *2023 IEEE 17th International Conference on Compatibility, Power Electronics and Power Engineering (CPE-POWERENG)*, 2023, pp. 1–6.

[10] A. U. Rahman, F. Pellitteri, N. Campagna, A. Di Tommaso, and R. Miceli, "Current Sharing Control of Multiphase Interleaving Single Inductor Four Switch Buck-Boost Converter for Energy Storage System," in *2024 IEEE 15th International Symposium on Power Electronics for Distributed Generation Systems (PEDG)*. IEEE, 2024, pp. 1–6.

[11] A. U. Rahman, N. Campagna, A. O. Di Tommaso, R. Miceli, A. Damiano, and A. Floris, "Advanced Control Analysis of Single Inductor Four Switch Non-Inverting Buck-Boost Converter for Energy Storage Units," in *2023 International Conference on Clean Electrical Power (ICCEP)*, 2023, pp. 267–272.

[12] A. Mishra, S. Mandal, J.-Y. Dieulot, M. Bachute, M. Faizan, A. Pinnarelli, M. Heidari, and A. Soleimani, "Non-Linear Control of Interleaved Boost Converter Using Disturbance Observer Based Approach," *IEEE Access*, 2025.

[13] S. V. Malge, M. G. Ghogare, S. L. Patil, A. S. Deshpande, and S. K. Pandey, "Chatter-free non-singular fast terminal sliding mode control of interleaved boost converter," *IEEE Transactions on Circuits and Systems II: Express Briefs*, vol. 70, no. 1, pp. 186–190, 2022.

[14] A. U. Rahman, F. Pellitteri, N. Campagna, A. O. D. Tommaso, and R. Miceli, "Decoupled Robust Backstepping Control of Multiphase Interleaving Converters for Power-to-Hydrogen Systems in DC Microgrids ," in *2024 IEEE 15th International Symposium on Power Electronics for Distributed Generation Systems (PEDG)*, 2024, pp. 1–6.

[15] R. Giral, L. Martinez-Salamero, R. Leyva, and J. Maixe, "Sliding-mode control of interleaved boost converters," *IEEE Transactions on Circuits and Systems I: Fundamental Theory and Applications*, vol. 47, no. 9, pp. 1330–1339, 2000.

[16] D.-Y. Jung, Y.-H. Ji, S.-H. Park, Y.-C. Jung, and C.-Y. Won, "Interleaved soft-switching boost converter for photovoltaic power-generation system," *IEEE Transactions on Power Electronics*, vol. 26, no. 4, pp. 1137–1145, 2010.

[17] D. Remoaldo, I. S. Jesus, and R. S. Barbosa, "Improved Fuzzy Incremental Conductance MPPT Algorithm for a Photovoltaic System," in *CONTROLO 2024*, A. P. Aguiar, P. Rocha Malonek, V. H. Pinto, F. A. C. C. Fontes, and R. Chertovskih, Eds. Cham: Springer Nature Switzerland, 2025, pp. 520–529.

[18] T. Qie, X. Zhang, J. Zhu, M. Vilathgamuwa, H. H. C. Iu, and T. Fernando, "A novel data-driven linear quadratic regulator for an interleaved DC/DC boost converter," *IEEE Transactions on Power Electronics*, vol. 39, no. 5, pp. 5400–5410, 2024.

[19] H. K. Khalil, *Nonlinear Systems*, 3rd ed. Upper Saddle River, NJ: Prentice Hall, 2002.